

CHARACTERIZATION OF CdTe THIN FILMS PREPARED BY STACKED LAYER METHOD

G. G. Rusu^{*}, M. Rusu, E. K. Polychroniadis^a, C. Lioutas^a

^{*}Al. I. Cuza “ University, Faculty of Physics, Blvd. Carol I, 11, 700506 Iasi, Romania

^aDepartment of Physics, Aristotle University of Thessaloniki, 54006 Thessaloniki, Greece

Nanocrystalline CdTe thin films ($d=300\text{nm} - 500\text{nm}$) deposited by thermal evaporation under vacuum using stacked layer method, onto glass substrates at room temperature were investigated. During the evaporation process, the substrate holder periodically passed, by rotational moving, over the CdTe evaporating source. The rotating frequency ($\nu = 20 - 210$ rpm) of the substrate holder and source temperature ($T_{\text{ev}} = 900 - 1200\text{K}$) during deposition have been considered as process parameters. The structural (surface morphology and film crystallinity), electrical (temperature dependence of conductivity) and optical (transmission and absorption spectra) properties of as deposited CdTe films are studied. The effect of heat treatment on the film structure is also investigated. The obtained results revealed an important influence of the above mentioned deposition parameters, especially the source temperature, on the film characteristics.

(Received July 4, 2005; accepted July 21, 2005)

Keywords: Cadmium telluride, Thin films, Electrical properties, Optical properties

1. Introduction

In the last years, the interest on the physical properties of the CdTe thin films have been considerable increased due to their practical importance in technology of thin-film devices as high-efficiency solar cells, field effect transistors, nuclear radiation detectors, etc. The quality of these devices is strongly influenced by the deposition techniques used for preparation of component films. A study of the correlation between physical properties of the CdTe films and their preparation conditions is still necessary for more comprehensive understanding of this correlation and for the improvement of the quality of these films for the technological applications. Various methods as hot wall vacuum evaporation, close-spaced sublimation, molecular beam epitaxy, electro-deposition, etc. have been used to prepare CdTe films [1–7]. Thermal evaporation in vacuum is also often used because it offers many possibilities to modify the deposition conditions and so to study the preparation conditions – physical properties relationships for respective films. It has been well established that in this preparation method the process parameters like substrate temperature, source temperature, deposition frequency (rate) change the quality and physical properties of the CdTe films [8 – 11].

In the present paper, the physical properties of CdTe films deposited in vacuum by stacked layer method have been investigated. The rotational rate of the substrate during film deposition and source temperature have been considered as process parameters and structural, electrical and optical properties of as deposited CdTe films are investigated.

2. Experimental

CdTe powder was thermally evaporated from a resistively heated tungsten crucible in a quasi-closed volume, onto glass substrates at room temperature. The residual pressure in standard

^{*} Corresponding author: rusugxg@uaic.ro

vacuum equipment was about 10^{-5} Torr. The substrates were fixed to a rotating disk periodically passing over the evaporation source with constant rate ν ranged between 20 rpm and 210 rpm. The source temperature, T_{ev} , maintained constant during film deposition, ranged from 900 K to 1200 K. The distance between film substrates and the evaporation source was approximately 7 cm. Other details of the preparation method and used experimental setup are given in our previous works [12, 13]. The interferometrically measured samples thickness, d , varied between 300 nm and 500 nm.

Some samples were heat-treated under ambient conditions for 20 min. at 620 K. The isochronal annealing arrangement was used.

The structural as well as morphological analysis were carried out by atomic force microscopy (AFM), X-ray diffraction (XRD) standard technique and by electron diffraction (ED).

Electrical conduction behavior of the obtained samples were investigated by measuring their electrical resistance in the temperature range 300 – 550 K, using surface type cells [14]. For electrical contacts, indium thin films electrodes deposited in vacuum onto CdTe films were used. The gap between electrodes was about 2 mm.

The optical reflectance and transmittance measurements were recorded in 500 – 1100 nm wavelength range using a STEAG-ETA OPTIK spectrometer. Optical measurements, corrected for the effect of the glass substrates, were used to calculate the absorption coefficient, α , and the optical energy gap, E_g^{opt} .

3. Results and discussion

3.1. Structural characterization

3.1.1. Surface morphology

Fig. 1 presents a selection of atomic force micrographs of the films deposited at various values for ν and T_{ev} , revealing a significant influence of these deposition parameters on the film surface morphology.

As it results from Fig. 1 (*Top*), the increase of rotational rate of the sample holder during deposition process at source temperature of 925 K, determines a greater uniformity of the film surface. As one can see, the surface of the film deposited with greater ν (210 rpm) shows more regular arrangement of the grains. The surface of such films contains a larger number of pyramidal shaped hillocks, homogeneously distributed on the film surface.

For the films deposited at higher source temperature (1165 K) with lower rotation rate ($\nu = 20$ rpm), the morphologic aspect of their surface is less pronounced, with very small grains and lower pores (Fig. 1 (*Bottom*)). The increase of ν up to 210 rpm, determines the growth on the film surface of some hillocks having a noticeable average sizes. An important increasing of the size of these hillocks takes place when the respective sample is heat-treated (Fig. 1 (d)). The presence on the film surface of such larger hillocks can be a consequence of the precipitation of the Te excess during deposition films. This conclusion is sustained by the results obtained by XRD and ED studies of such films (see § 3.1.2).

For a surface area of $1 \times 1 \mu\text{m}^2$ the average roughness (a-r) and the root mean square surface (rms) roughness for some representative samples deposited in various conditions have been calculated. The (a-r) roughness (the average deviation of height data from the average of the data) was calculated with the relation [15]:

$$R_{a-r} = \frac{\sum_{n=1}^N |z_n - \bar{z}|}{N} \quad (1)$$

where \bar{z} is the mean z height and N the number of pixels in the image region. The rms roughness (or standard deviation of the height data) was determined using standard definition [15]:

$$R_{rms-r} = \sqrt{\frac{\sum_{n=1}^N (z_n - \bar{z})^2}{N - 1}} \quad (2)$$

Table 1 summarizes the calculated values for R_{a-r} and R_{rms-r} for CdTe samples from Fig. 1.

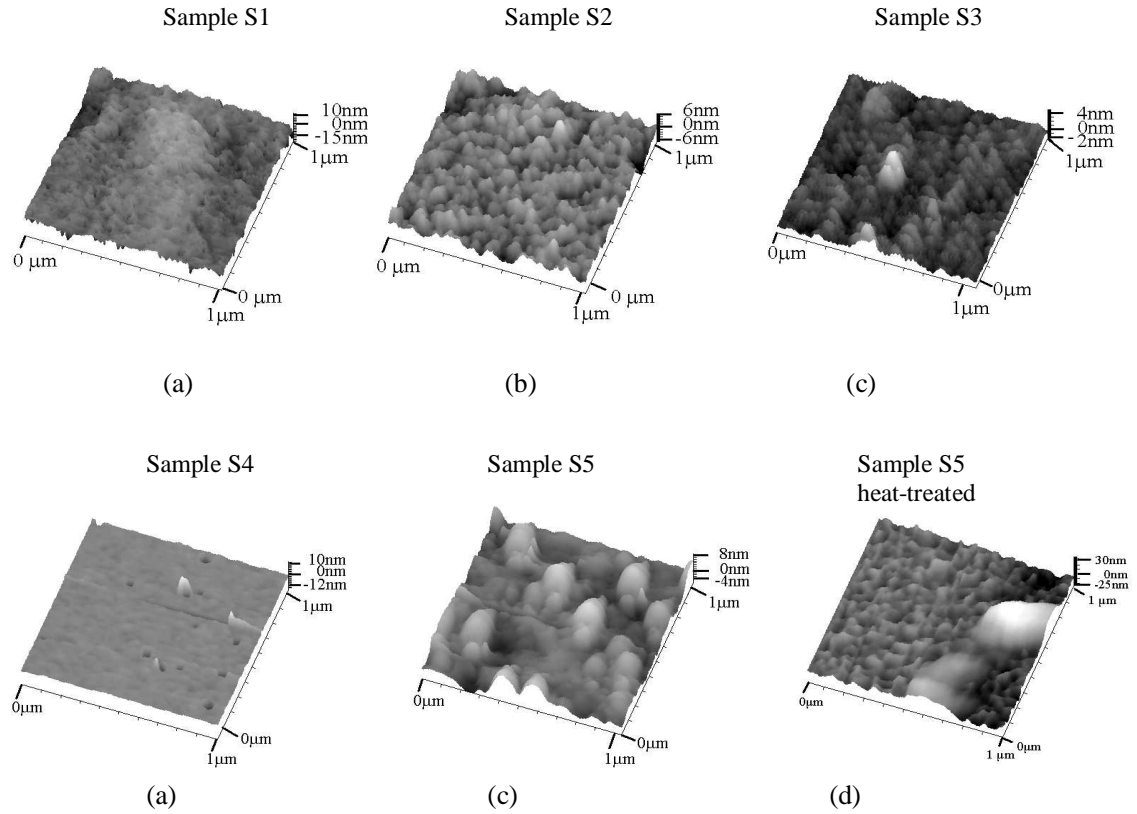


Fig. 1. AFM topography for CdTe films deposited with different values for ν : (a) 20 rpm; (b) 120 rpm; (c) 210 rpm. *Top*: at source temperature of 925 K; *Bottom*: at source temperature of 1165 K; (d) sample S5 after heat treatment (the sample thicknesses are listed in Table 1).

Table 1. Values of average roughness and rms roughness for CdTe films deposited at different values of source temperature (T_{ev}) and rotational rate (ν); d – film thickness; D – average CdTe crystallite size in [111] direction calculated from XRD patterns.

Sample	d (nm)	T_{ev} (K)	ν (rpm)	a-r (nm)	rms-r (nm)	D (nm)
S 1	340	925	20	2.31	3.03	22.0
S 2	420	925	120	0.95	1.21	28.3
S 3	360	925	210	0.57	0.79	20.6
S 4	390	1165	20	0.53	1.04	10.5
S 5	475	1165	210	2.12	2.79	16.5
S 5 heat treated	475	1165	210	8.48	12.86	57.6

From the Table 1 clearly results the tendency of the roughness of the films deposited at lower source temperature to decrease with increasing of the rotational rate. In contrast, at greater source temperature, the increasing of rotational rate determines an increasing of the film roughness.

3.1.2. X-ray diffraction studies

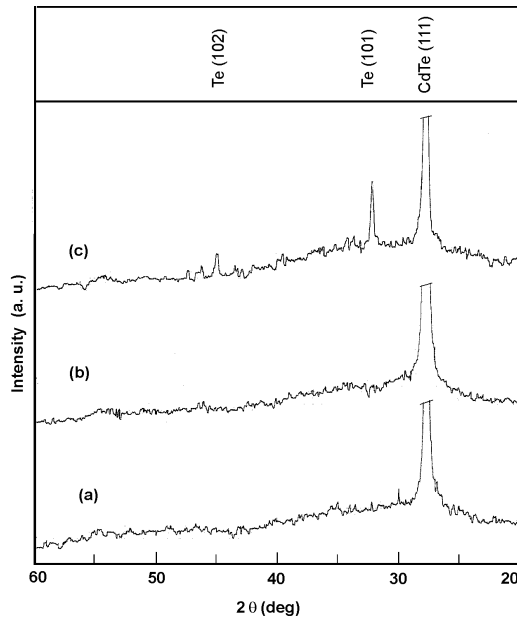


Fig. 2. XRD patterns for CdTe films deposited at source temperature of 925 K, with different values for ν : (a) 20 rpm (sample S1); (b) 210 rpm (sample S3), (c) sample S3 after heat treatment.

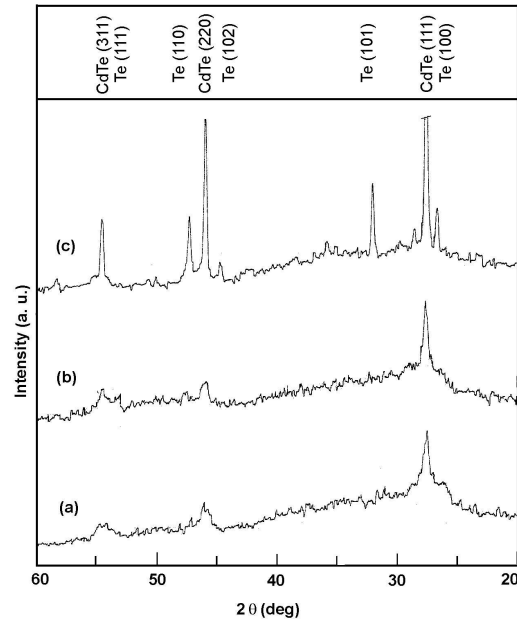


Fig. 3. XRD patterns for CdTe films deposited at source temperature of 1165 K, with different values for ν : (a) 20 rpm (sample S4); (b) 210 rpm (sample S5); (c) sample S5 after heat treatment.

The structure of as-deposited films was investigated using XRD technique, with $\text{CoK}\alpha$ radiation ($\lambda = 0.1790$ nm) in the range 20° – 60° . In Figs. 2, 3 representative XRD patterns for studied films are shown. It may be observe that for the films deposited at source temperature of 925 K, the diffraction patterns yield only a sharp and intense (111) reflection at $2\theta \cong 27.7^\circ$ (Fig. 2 (a,b)). This indicates that in these films the CdTe microcrystallites grow preponderantly with (111) planes parallel to the substrates. The rotational rate, ν , does not essentially influence this structure. After heat-treatment these films present the same (111) texture. In the case of the heat-treated films deposited at $T_{\text{ev}} = 925$ K but with increased ν (210 rpm), their XRD patterns exhibit additional peaks for Te at $2\theta \cong 32.1^\circ$ and $2\theta \cong 44.8^\circ$. This indicates that the respective films exhibit an amount of tellurium excess that precipitates during annealing process (Fig. 2c).

For the samples deposited at greater source temperature ($T_{\text{ev}} = 1165$ K), the XRD patterns exhibit the weak broad peaks at $2\theta \cong 27.7^\circ$, 46.1° and 54.6° , which correspond to reflection on (111), (220) and (311) planes of CdTe cubic structure, respectively, along with additional shallow diffraction peaks of low intensity which are characteristic for Te, at $2\theta \cong 47.3^\circ$ and $2\theta \cong 53.8^\circ$ (Fig. 3 (a,b)). This means that the films contain an admixture of fine-grained CdTe and Te.

When such films are annealed at temperature of 620 K, their structure becomes polycrystalline without any preferred orientation. Also, another peaks for Te at $2\theta \cong 26.8^\circ$, 32.1° and 44.8° respectively are visible in respective pattern (Fig. 3c). The increase of the intensities of the Te diffraction peaks after heat treatment, indicates that the average size of Te crystallites in respective films increased as consequence of the heat treatment. This is in agreement with AFM micrograph from Fig. 1 (d).

The CdTe average crystallite size in [111] direction were evaluated for discussed samples using the relation [16]:

$$D = \frac{0.9\lambda}{\beta \cos \theta} \quad , \quad (3)$$

where D is the average crystallite size in normal direction to the reflection plane, θ - the Bragg angle and β - the corrected full width at half maximum [FWHM]. As it results from Table 1, D depend

both on rotational rate, ν , and source temperature, T_{ev} , the lower source temperature determining a greater crystallite sizes. The heat treatment of the samples deposited at 1165 K determines an important increase of CdTe crystallite size.

3.1.2. Electron microscopy studies

The electron diffraction (ED) studies on the structure of the investigated samples confirm above presented results. Fig. 4a presents a typical ED pattern for as deposited sample at $T_{ev} = 1165$ K and $\nu = 20$ rpm. As it can be seen from Fig. 4, the respective ED pattern presents symmetrical rings of spots that reveal the polycrystalline structure of the film. The analysis of the diffraction patterns shown the co-existence of two phases. The calculation of the interplanar distances from ED patterns shown that the main phase is cubic and is in very good agreement with those of the FCC CdTe (PDF #15-0770), with cell parameters $a = 0.6481$ nm (Fig. 4 b).

Additional individual spots in positions not predicted from the above mentioned phase (indicated with small arrows) may be seen on Fig. 4a. These extra spots can be attributed to the tellurium excess in respective sample. In Fig. 4c the intensity distribution obtained from digitized images for a direction containing the extra spot and the estimated positions of the rings on the ED pattern (inset) for hexagonal Te (with cell parameters $a = 0.4457$ nm and $c = 0.5927$ nm) (PDF # 36-1452), are shown. As it may be seen, the positions of the observed spots are in good agreement to the calculated ones, fact that reveals the presence of Te microcrystallites in films.

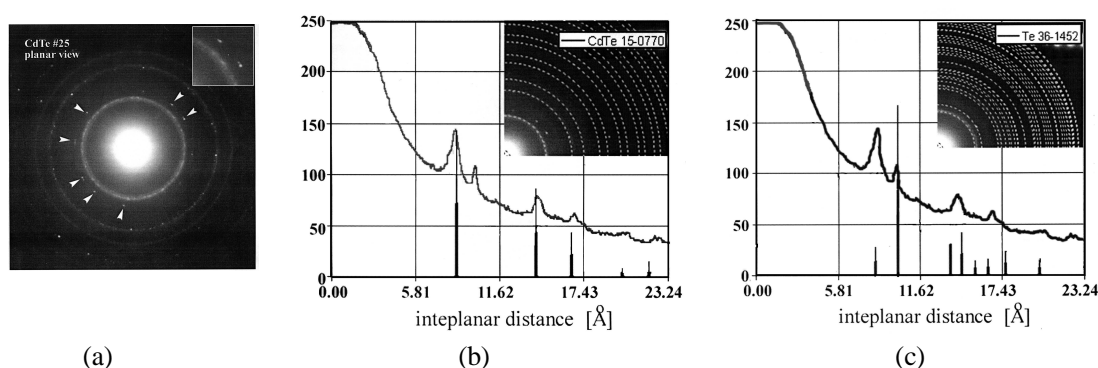


Fig. 4. (a) typical ED pattern of the films deposited at 1165 K (small arrows indicate the position of the extra spots); (b, c) the relative spot intensity on the intensity distribution for direction containing the extra spot. Inset: estimated positions of the rings on the ED pattern for CdTe phase (b) and Te phase (c).

Thus, both the X-ray patterns and ED studies confirm the presence of Te excess in CdTe studied films.

3.2. Electrical properties

It is well known that the electronic transport properties of the polycrystalline thin films strongly depend on their structure [17]. The study of the temperature dependence of electrical conductivity of such films offers a lot of information on the electrical conduction mechanism in respective films in correlation with their structure. Our previous studies revealed that CdTe film structure may be changed in first heating cooling cycle during such electrical measurements [13, 14]. From this reason, in this paper, for the study of the temperature dependence of electrical conductivity, the samples were previously subjected to a heat treatment consisting in several successive heating and cooling cycles in the temperature range 300 – 620 K. In this way, CdTe films with stabilized structure and reproducible electrical properties were analyzed. In the Figs. 5, 6, the typical temperature dependence of electrical conductivity, σ , for as heated films, prepared at

different deposition parameters are shown. It can be observed a linear dependence of $\ln \sigma$ vs. $10^3/T$ for all studied samples. This suggest that σ varies with the temperature according to the relation:

$$\sigma = \sigma_0 \exp(-\Delta E / kT) \quad , \quad (4)$$

which is in concordance with the thermally activated conduction mechanism [17]. In the relation (4), ΔE denotes the thermal activation energy of electrical conduction, σ_0 represents a parameter depending on the semiconductor nature and k is the Boltzmann's constant. The activation energy values, ΔE , calculated from the slope of $\ln \sigma$ vs. $10^3/T$ curves from Figs. 5, 6 are given in Table 2. It may be seen that at constant source temperature, the thermal activation energy decreases with increase of rotational rate, ν . Also, an important decrease of ΔE is determined by increase of source temperature. These results may be correlated with Te excess that is greater in respective CdTe films. The segregation of tellurium excess in such films may determine the decrease of potential barrier in the grain boundary region and hence a decrease of ΔE [17].

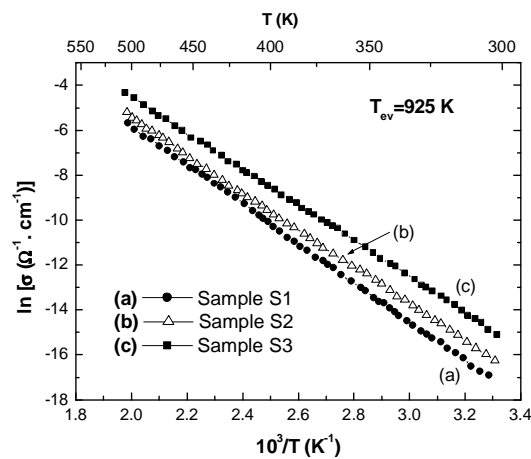


Fig. 5. Typical temperature dependence of electrical conductivity for CdTe films deposited at $T_{ev} = 925$ K with various rotational rate: (a) $\nu = 20$ rpm; (b) $\nu = 120$ rpm; (c) $\nu = 210$ rpm

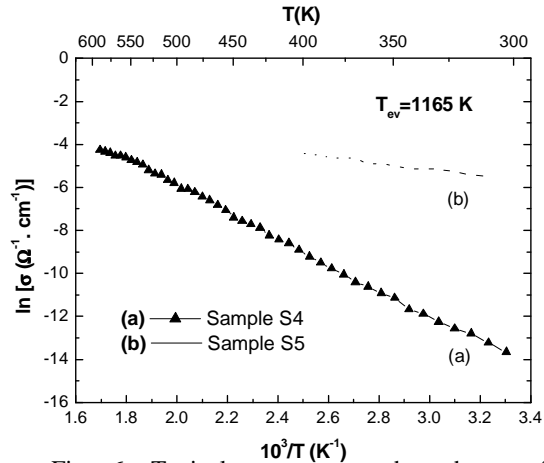


Fig. 6. Typical temperature dependence of electrical conductivity for CdTe films deposited at $T_{ev} = 1165$ K with various rotational rate: (a) $\nu = 20$ rpm; (b) $\nu = 210$ rpm.

Table 2. Some electrical and optical characteristics for the typical studied samples d – film thickness; T_{ev} – source temperature; ν – rotational rate; ΔE – thermal activation energy, σ_c – electrical conductivity at room temperature after heat treatment; E_g^{opt} – optical band gap.

Sample	d (nm)	T_{ev} (K)	ν (rpm)	σ_c ($\Omega^{-1} \cdot \text{cm}^{-1}$)	ΔE (eV)	E_g^{opt} (eV)
S1	340	925	20	4.6×10^{-8}	0.75	1.54
S2	420	925	120	8.8×10^{-8}	0.71	1.53
S3	360	925	210	2.7×10^{-7}	0.68	1.52
S4	390	1165	20	1.1×10^{-6}	0.52	1.42
S5	475	1165	210	4.1×10^{-3}	0.14	1.34

In Table 2, the electrical conductivity at room temperature, σ_c , for typical heat treated samples are also indicated. One can be observe the increase of σ_c with increase of ν and T_{ev} , hence with increase of Te contents in the films. This can be explained by the role played by the free Te atoms in CdTe lattice like the acceptor impurities in p type semiconductors [18]. An increase of the Te amount will determine an increase of carrier concentration and, consequently, an increase of the electrical conductivity of the film [18, 19].

3.3. Optical properties

The absorption coefficients, α , of the as-deposited CdTe films were determined by measuring the transmittance, T , and the reflectance, R , in the wavelength range of CdTe absorption edge, using the relation [20]:

$$\alpha = \frac{1}{d} \ln \left[\frac{(1-R)^2}{T} \right] \quad , \quad (5)$$

where d denotes the film thickness.

Fig. 7 shows typical absorption spectra for CdTe films deposited at different values for ν and T_{ev} . It can be observe that the source temperature is the main factor which influences the film absorbance. The greater values of α for samples deposited at 1165 K can be attributed to the stronger absorbance of tellurium in analyzed spectral range [13].

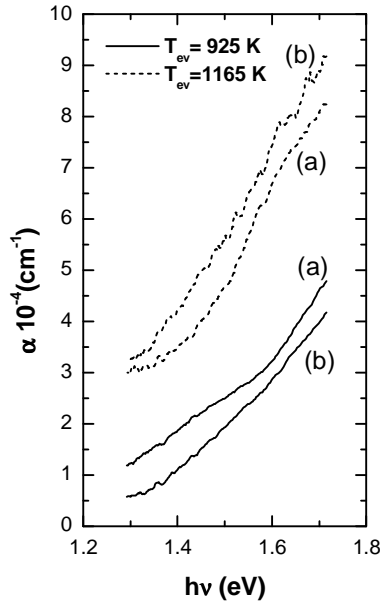


Fig. 7. Absorption spectra for studied CdTe films: (a) $\nu = 20$ rpm; (b) $\nu = 210$ rpm.

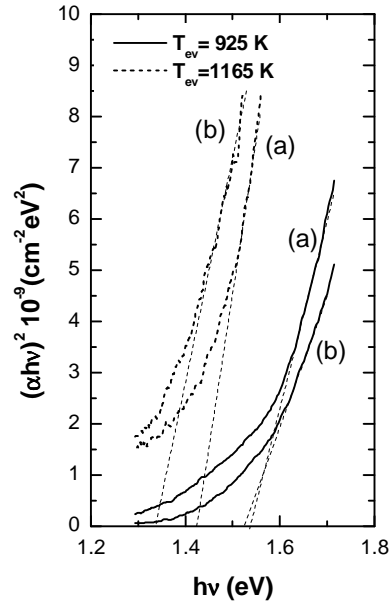


Fig. 8. The dependence $(\alpha h\nu)^2 = f(h\nu)$ corresponding to samples from Fig. 7.

From the optical absorption spectra, by assuming allowed direct inter-band transitions [18], the optical band-gap, E_g^{opt} , were determined by extrapolating the linear portion of the $(\alpha h\nu)^2 = f(h\nu)$ plots to $(\alpha h\nu)^2 = 0$. Fig. 8 shows the $(\alpha h\nu)^2$ vs. $h\nu$ for different samples. The obtained optical direct band-gap values, for respective samples are also listed in Table 2. The values of about 1.5 eV obtained for samples deposited at $T_{ev} = 925$ K are in good agreement with those found in the literature data for the CdTe band-gap. The lower values of E_g^{opt} obtained for samples deposited at $T_{ev} = 1165$ K can be correlated with greater Te amount present in respective films. This may thereby increases the number of non-saturated bonds in grain boundary, and so to perturb the band structure. The high concentration of the acceptor states introduced by these free Te atoms give rise to the density of the state tails extending into the forbidden band. Consequently, the effective band-gap width will be reduced [8, 21].

4. Conclusions

CdTe thin films were deposited in vacuum onto unheated rotating glass substrates at different CdTe source temperatures. The study of the structure, electrical and optical properties of as deposited films revealed that the rotating rate influence primarily the morphology and crystallinity of

the films whereas the source temperature is the most important factor in determining of the electrical and optical properties. An increase of the rotational rate and source temperature favor the increasing of the tellurium excess in CdTe films, playing an essential role in determining both of the electrical conductivity and optical absorbance of CdTe films. As the amount of free Te atoms increases, the electrical conductivity decreases from $4.6 \times 10^{-8} \Omega^{-1} \text{cm}^{-1}$ to $4.1 \times 10^{-3} \Omega^{-1} \text{cm}^{-1}$ and optical band-gap varies in the range 1.50 eV - 1.34 eV.

Acknowledgements

Part of this work was made inside the Scientific Cooperation Project AUF (Agence Universitaire de la Francophonie) No. 6301PS 429/2004.

References

- [1] S. M. So, W. Hwang, P. V. Meyers, C. H. Liu, J. Appl. Phys. **61**, 2234 (1987).
- [2] M. Bouroushian, Z. Loizos, N. Spyrellis, G. Maurin, Thin Solid Films **229**, 101 (1993).
- [3] N. El-Kadry, A. Ashour, S.A. Mahmoud, Thin Solid Films **269**, 112 (1995).
- [4] A. I. Oliva, E. Anguiano, M. Aguilar, R. Castro-Rodriguez, J. L. Peña, J. Matter. Sci., Mater. Electron. **6**, 154 (1995).
- [5] N. Romeo, A. Bosio, R. Tedeschi, V. Canevary, Mat. Chem. Phys. **66**, 201 (2000).
- [6] X. Mathew, J. Phys. D: Appl. Phys. **33**, 1565 (2000).
- [7] R. K. Sharma, G. Singh, A.C. Rastogi, Sol. Energy Mater. Sol. Cells **82**, 1-2, 201 (2004).
- [8] R. Chakrabarti, S. Ghosh, S. Chaudhuri, A.K. Pal, J. Phys. D: Appl. Phys. **32**, 1258 (1999).
- [9] L. R. Cruz, R. R. de Avillez, Thin Solid Films **373**, 15 (2000).
- [10] J. H. Lee, D. G. Lim, J. S. Yi, Sol. Energy Mater. Sol. Cells **75**, 1-2, 235 (2003).
- [11] S. Lalitha, R. Sathyamoorthy, S. Senthilarasu, A. Subbarayan, K. Natarajan, Sol. Energy Mater. Sol. Cells, **82**, 1-2, 187 (2004).
- [12] M. Rusu, I. I. Nicolaescu, G. G. Rusu, Appl. Phys. **A 70**, 565 (2000).
- [13] G. G. Rusu, J. Optoelectron. Adv. Mater. **3**, 861 (2001).
- [14] G. G. Rusu, M. Rusu, Solid State Commun. **116**, 363 (2000).
- [15] M. Aguilar, A. I. Oliva, R. Castro-Rodriguez, J. L. Peña, Thin Solid Films **293**, 149 (1997).
- [16] H. P. Klug, L. E. Alexander, X-ray Diffraction Procedures for Polycrystalline and Amorphous Materials, 2nd edition, (Wiley, New York, 1974).
- [17] L. L. Kazmersky (Ed.) Polycrystalline and Amorphous Thin Films and Devices, (Academic Press, New York-London, 1980).
- [18] R. Bangava (Ed.), Properties of Wide Bandgap II-VI Semiconductors, (INSPEC, IEE, Herts, UK, 1996).
- [19] J. Felix-Valdez, C. Falcony, M. Tufino, C. Menezes, J.M. Dominguez, A. Garcia, J. Appl. Phys. **61**, 5076 (1987).
- [20] T. S. Moss, G.J. Burrell, B. Ellis, Semiconductor Opto-Electronics, (Butterworth & Co Ltd., London, 1973).
- [21] J. I. Pankove, Optical Processes in Semiconductors, (Dover, New York, 1971).